

See discussions, stats, and author profiles for this publication at: <https://www.researchgate.net/publication/231216654>

Redox Properties and Mössbauer Spectroscopy of *Azotobacter vinelandii* Bacterioferritin

ARTICLE *in* BIOCHEMISTRY · JULY 1986

Impact Factor: 3.02 · DOI: 10.1021/bi00363a023

CITATIONS

59

READS

22

5 AUTHORS, INCLUDING:



[Gerald D Watt](#)

Brigham Young University - Provo Main Campus

134 PUBLICATIONS 2,535 CITATIONS

SEE PROFILE



[Richard B. Frankel](#)

California Polytechnic State University, San L...

345 PUBLICATIONS 12,831 CITATIONS

SEE PROFILE



[Georgia Papaefthymiou](#)

Villanova University

153 PUBLICATIONS 6,865 CITATIONS

SEE PROFILE

Redox Properties and Mössbauer Spectroscopy of *Azotobacter vinelandii* Bacterioferritin[†]

G. D. Watt,* R. B. Frankel,[‡] G. C. Papaefthymiou,[‡] K. Spartalian,[§] and E. I. Stiefel^{||}

Battelle-Kettering Laboratory, Yellow Springs, Ohio 45387

Received January 14, 1986; Revised Manuscript Received March 26, 1986

ABSTRACT: Biochemical characterization, redox measurements, and Mössbauer spectral data of reduced and oxidized bacterial ferritin from *Azotobacter vinelandii* are reported. Ferritin samples ranging from 600 to 2400 Fe atoms/molecule were obtained from bacterial cells grown 20 and 40 h. The bacterial ferritin contained an average of 1.4 Fe/P_i and 0.5 *b*-type heme/subunit. Reduction potentials of -475 mV for heme reduction and -420 mV for core iron reduction were determined, the latter value being apparently independent of pH. Apobacterioferritin (containing only heme) has a reduction potential of -225 mV, a value 250 mV more positive than when the core is present. Mössbauer spectra of oxidized and partially reduced bacterial ferritin clearly show discrete Fe³⁺ and Fe²⁺, the former in an antiferromagnetically coupled structure. Blocking temperatures are lower for bacterial ferritin than for mammalian ferritin. The parameters for Fe²⁺ in bacterial ferritin are similar to those in reduced mammalian ferritin.

The recent discovery (Bulen et al., 1973) and characterization (Stiefel & Watt, 1979; Yaviv et al., 1981) of bacterial proteins possessing many properties in common with the more thoroughly studied mammalian ferritins have prompted a more detailed comparison of these two types of iron core containing proteins.

As was previously noted (Stiefel & Watt, 1979), both proteins are composed of 24 subunits of 17 000–20 000 daltons each with a similar amino acid composition. Both proteins are capable of accommodating up to 4000 Fe atoms in their interior cavities. However, certain properties of the bacterial proteins make them unique. In particular, both the *Azotobacter vinelandii* (Av) ferritin and *Escherichia coli* (Ec) ferritin contain low potential *b*-type heme groups which are absent from all well-characterized mammalian, plant, and fungal ferritins. Also, the iron-containing core of Av ferritin was reported (Stiefel & Watt, 1979) to undergo reduction in which each Fe³⁺ ion originally present was converted to Fe²⁺ and retained within the bacterioferritin core. The *b*-type heme present in the protein also is reduced under these conditions with a redox potential only slightly more negative than the core iron atoms (Stiefel & Watt, 1979). Initially, it was thought that this reducibility of each core iron atom in bacterial ferritin, with complete retention as Fe²⁺, was unique to Av ferritin. However, our recent redox measurements (Watt et al., 1985) on horse spleen ferritin, in the absence of iron chelators, have demonstrated a similar capability with this mammalian system. These latter redox reactions displayed a well-defined decrease of the reduction potential with increasing pH, suggesting that proton transfer accompanied electron transfer during core reduction.

Mössbauer spectra of partially reduced mammalian ferritin established discrete Fe²⁺ and Fe³⁺ components at concentrations consistent with the degree of core reduction. The Fe³⁺ component of the partially reduced samples displayed magnetic hyperfine interaction at low temperature nearly identical with the native oxidized samples (Watt et al., 1985), suggesting that reduction to Fe²⁺ is localized within each molecule (perhaps on the surface of the core) or, more likely, that reduction occurs first with specific components of the polydisperse solution (perhaps the low iron containing molecules) used in the measurements.

These Mössbauer results and redox data on mammalian ferritin prompted us to carry out similar detailed studies on the Av protein so that a comparison can be made of the core reduction properties and the environments of the Fe³⁺ and Fe²⁺ in these two systems. As we will show, there are significant differences in the chemical composition and redox behavior of the mineral cores of these two proteins. In addition, we have found that the presence of the iron core has a significant effect on the redox properties of the heme groups present in apo- and holobacterioferritin.

MATERIALS AND METHODS

Av ferritin was isolated from *Azotobacter vinelandii* cells grown to mid-log phase (20 h) and to near-stationary phase (40 h) as previously described by Bulen et al. (1973). The isolated protein was recrystallized 3 times, and the total iron, inorganic phosphate (P_i), and heme contents were determined. Total protein for either holo or apo Av ferritin was measured by complete amino acid analysis against which Lowry and Biuret methods were calibrated for routine protein measurements. Apo bacterial ferritin was prepared by a scaled-down modification of the thioglycolic method used for preparation of apo mammalian ferritin (Treffry & Harrison, 1978).

Microcoulometric reduction measurements of Av ferritin were carried out as previously described (Watt, 1979) at pH 7.0, 8.0, and 9.0 using 50–75 μ M methyl viologen or benzyl viologen as mediators in 0.05 M tris(hydroxymethyl)amino-methane (Tris) or 0.05 M 2-[[tris(hydroxymethyl)methyl]-amino]ethanesulfonic acid (TES) containing 0.25 M NaCl. Reduction potentials and *n* values were obtained from the

[†] R.B.F. and G.C.P. were partially supported by the Office of Naval Research. The Francis Bitter National Magnet Laboratory is supported by the National Science Foundation. G.D.W. was supported by Project PCM-8207775 from the National Science Foundation.

[‡] Present address: Francis Bitter National Magnet Laboratory, Massachusetts Institute of Technology, Cambridge, MA 02139.

[§] Present address: Department of Physics, The University of Vermont, Burlington, VT.

^{||} Present address: Corporate Research Science Laboratory, Exxon Research and Engineering Co., Clinton, NJ.

Table I: Analytical Data for Av Bacterioferritin Samples

Av ferritin	[Av ferritin](mg/mL)	μmol of P_i/mg	μmol of heme/mg	μmol of Fe/mg	Fe/ P_i ratio	heme/subunit ^b	Fe/Av ferritin ^c
1	14.4	1.63	0.024	2.50	1.5	0.45	1080
2	6.8	2.10	0.022	2.80	1.6	0.43	1210
3	8.1	1.92	0.030	2.72	1.4	0.54	1175
4	6.1	1.76	0.030	2.31	1.3	0.54	998
5	7.1	1.78	0.027	2.05	1.1	0.49	886
6	4.2		0.024	4.20		0.45	1814
7 ^a	3.9	0	0.027	0.030		0.49	11.8

^a Av apoferritin. ^b Calculated by assuming 17 125 daltons per subunit. ^c Calculated by assuming M_r 411K ($24 \times 17 125$).

resulting plots of percent reduction of Av ferritin as a function of applied reducing potential. Because the core iron/heme ratio was >100 in the Av samples used, the microcoulometric method results represent essentially core iron reduction only. Spectroelectrochemical measurements of reduced heme development as a function of applied potential were made in a stirred 1.0-cm path-length cuvette containing a large-area platinum gauze electrode attached to the nonoptical faces of the cuvette and controlled by a PAR 174 potentiostat. The increase in intensity of the heme α -band at 557.5 nm was plotted against the applied electrode potential to obtain the reduction potential of the heme component only of Av ferritin. Minor absorbance corrections due to the presence of the mediator and residual absorbance of the core iron at this wavelength were made. All electrochemical measurements were made relative to the saturated calomel electrode (SCE) but were corrected and are reported here relative to the normal hydrogen electrode (NHE).

Reductive optical titrations of Av ferritin with standardized $\text{S}_2\text{O}_4^{2-}$, standardized $\text{S}_2\text{O}_4^{2-}$ containing 50 μM methyl viologen, and electrochemically reduced methyl viologen were carried out in anaerobic 1.0-cm quartz cuvettes. Optical spectra were recorded on a Cary 118 spectrophotometer in the 300–800-nm range.

Mössbauer measurements were made on approximately 20 mg/mL oxidized and partially reduced Av bacterioferritin samples containing naturally abundant ^{57}Fe (2.2%) in air-tight plastic containers. Partially reduced samples were passed through a Sephadex G-25 column in an inert atmosphere to remove non-ferritin-bound Fe^{3+} and Fe^{2+} ions and frozen immediately thereafter.

Bacterioferritin samples for both the optical and Mössbauer spectroscopic measurements were prepared in 0.05 M Tris and 0.05 M TES containing 0.1 M NaCl. No evidence of buffer-dependent spectroscopic effects was observed in either the core or the heme properties.

RESULTS

Table I contains analytical data regarding the core composition and heme content of six separately prepared Av ferritin samples. Columns 3, 4, and 5 present inorganic phosphate (P_i), heme, and Fe content per milligram of Av ferritin, respectively, the latter having been obtained from total amino acid analysis. The last three columns present the Fe/ P_i ratio, heme content per 17 125-dalton subunit, and Fe content per 24-subunit molecule, respectively. Several important compositional features of Av ferritin are to be noted.

First, the phosphate content of the Av ferritin samples listed in Table I is quite high, averaging about 800 P_i /Av ferritin molecule. P_i is clearly a significant component of the Av ferritin core, occurring at a concentration near 80% that of the iron present. The data in Table I average 1.4 Fe/ P_i , a value considerably different from 9.0 obtained from mammalian ferritin possessing a core with the average composition

of $(\text{FeO}\cdot\text{OH})_8\text{FeO}\cdot\text{OPO}_3\text{H}_2$. On a compositional basis, the iron-containing cores of Av ferritin and mammalian ferritin are distinctly different.

The second feature of interest is the presence of heme in the bacterial ferritins and its absence in other ferritins. The heme content of the Av ferritin samples in Table I was measured in the presence of formic acid using hemin and hemoglobin as standards under the same conditions. The results in Table I give an average value of 0.026 μmol of heme/mg of Av ferritin, a result independent of the degree of iron loading of the protein. Using 17 125 as the subunit molecular weight, we calculate an average value of 0.49 heme/subunit for Av ferritin.

It is interesting to note that Av ferritin isolated from cells grown to mid-log phase (20 h) contained 600–1000 Fe atoms/ferritin while ferritin isolated from cells in stationary phase (40 h) contained 1200–2000 Fe atoms/ferritin. Although considerable variability in iron content was encountered in Av ferritin isolated from cells grown under the two sets of conditions, it was generally observed that ferritin obtained from the more rapidly growing cells contained less iron than that obtained from cells grown to near-stationary phase. In addition, electron microscopy and ultracentrifugation studies both clearly indicate the polydisperse nature of the iron-containing cores in Av ferritin. In the experiments to be discussed, we have examined Av ferritin samples containing from 600 to 2400 Fe atoms/Av ferritin and have observed no effect attributable to this iron variability in the properties of the core that our experiments have probed. However, some differences between holo and apo Av ferritin were noted and will be discussed in more detail in a later section.

Chemical Reduction of Core Fe^{3+} . The addition of $\text{S}_2\text{O}_4^{2-}$ to anaerobic Av ferritin at concentrations such that the $\text{S}_2\text{O}_4^{2-}/\text{Fe}^{3+}$ ratio was 0.5 (1 e^-/Fe^{3+}), 3.0 (6 e^-/Fe^{3+}), and 10 (20 e^-/Fe^{3+}) resulted in only a slow (several hours) reduction reaction of Av ferritin as monitored at 557 nm (the heme α -band) and 480 nm (a region characteristic of the Fe^{3+} core iron atoms). The slow development of the heme band occurred concomitantly with the slow decrease in absorbance of the core iron, suggesting that both types of redox centers were undergoing reduction at essentially the same low rate. The addition of methyl viologen (MV), a cationic, one-electron mediator, greatly increases the rate of Av ferritin reduction as monitored at the indicated wavelengths, with the reaction going to completion in less than 10 min. Most chemical reduction reactions reported here were carried out with standardized, reduced methyl viologen or standardized $\text{S}_2\text{O}_4^{2-}$ containing catalytic amounts of this mediator to facilitate the reduction.

Figure 1 is an optical titration of Av ferritin with standardized, electrochemically reduced MV monitored at 557 nm (the heme α -band) and 480 nm (a spectral position representative of the Fe^{3+} core). It is seen that successive additions of MV cause an immediate and monotonic decrease in the

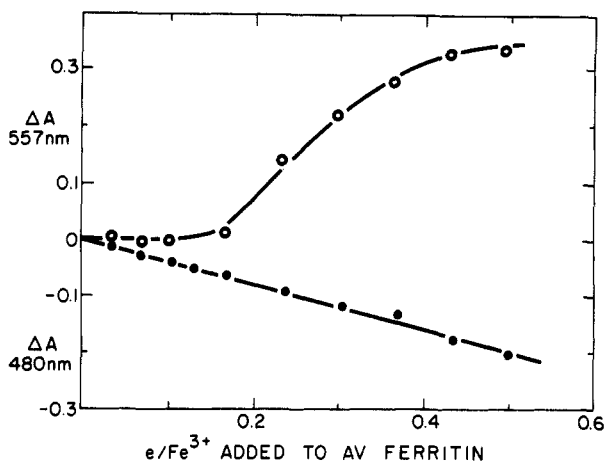


FIGURE 1: Reduction titration of Av ferritin with reduced methyl viologen, monitored at 557 nm for heme development (O) and at 480 nm for core iron reduction (●).

optical absorption of the core Fe^{3+} as it undergoes conversion to Fe^{2+} as monitored at 480 nm. However, when heme development at 557 nm is concurrently monitored, it is seen that heme reduction is not detectable until $\sim 15\%$ of the core Fe^{3+} has been reduced. The Av ferritin sample used in Figure 1 contained an average of 1876 Fe atoms/molecule so that an average of ~ 300 Fe^{3+} ions had undergone reduction within the core before reduced heme development became evident. After this degree of core reduction has occurred, heme development and core Fe^{3+} reduction then occur together to the limit of $\sim 50\%$ total reduction where the experiment was terminated. It is not feasible to proceed beyond 50% reduction using methyl viologen as a reductant because the reduction potential of the Fe^{3+} -containing core and that for methyl viologen are very similar and the latter therefore does not possess the electromotive capacity, by itself, for complete and stoichiometric reduction of the core Fe^{3+} in Av ferritin. Complete reduction of Av ferritin can be accomplished electrochemically or by using the stronger $\text{S}_2\text{O}_4^{2-}$ reductant combined with a mediator level concentration of methyl viologen. Titrations carried out with this system yield results identical with those shown in Figure 1. The $\text{S}_2\text{O}_4^{2-}$ -MV system has the disadvantage that as reduction proceeds to near completion, SO_3^{2-} , a redox byproduct of the $\text{S}_2\text{O}_4^{2-}$ reaction, reaches concentrations equivalent to the Fe^{2+} produced during reduction. Although SO_3^{2-} is not a particularly strong Fe^{2+} chelator, its high concentration combined with its weak Fe^{2+} chelating ability results in some Fe^{2+} loss when $\text{S}_2\text{O}_4^{2-}$ is used as a reductant for Av ferritin.

Fe^{3+} Core Reduction Potential. The reduction potential of Av ferritin as determined by microcoulometry was previously reported (Stiefel & Watt, 1979) to be -416 mV (NHE) at pH 8.0. The protein used in this previous study contained an average of 1600 Fe^{3+} /molecule, and each Fe^{3+} present underwent a one-electron reduction as shown by an $n = 1$ value derived from the reduction curve as well as a one-electron reduction value obtained from electron counting by coulometric methods (Watt, 1979). This result has been verified by using 10 separately prepared Av ferritin samples ranging in iron content from 600 to 2400 Fe^{3+} /ferritin. Reduction potentials of -420 ± 20 mV and coulometrically determined e^-/Fe^{3+} values of 0.83–1.10 were determined at pH 7.0 for all samples. In addition, reduction potentials of representative Av ferritin samples were measured at pH 7.0, 8.0, and 9.0 and found to be invariant with a reduction potential of -420 ± 20 mV. At pH 6.0, a positive shift to -390 mV was observed, suggesting the onset of a proton-linked reduction process in which electron

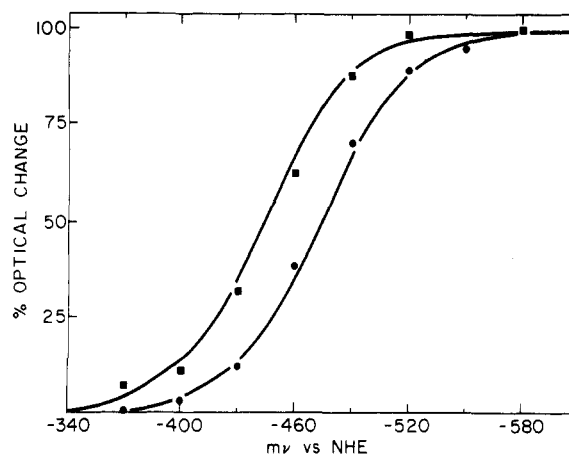


FIGURE 2: Redox potentials of heme (●) and core iron (■) measured in a stirred spectroelectrochemical cuvette.

transfer to the core iron atoms is accompanied by proton uptake.

The microcoulometric method just described measures the total charge transferred to Av ferritin, but because the heme iron is present to the extent of only 1–2% of the total iron, its redox properties are difficult to determine by this procedure in the presence of the core iron. The microcoulometric method thus provides an accounting of total electrons transferred to the Av ferritin (one electron for each iron present) and a redox potential for the dominant form of iron present.

To gain detailed redox information about the two separate types of redox centers present (the core Fe^{3+} and the heme groups) in Av ferritin, spectroelectrochemical methods (Heineman, 1980; Watt, 1979) were employed. The development of the reduced heme α -band at 557 nm and the decrease in absorbance at 480 nm, corresponding to core Fe^{3+} reduction, were simultaneously monitored spectrophotometrically as a function of applied reduction potential in a spectroelectrochemical cell. Figure 2 displays the percent increase in absorbance at 557 nm arising from Av ferritin heme reduction and the percent decrease in absorbance at 480 nm arising from core Fe^{3+} reduction as a function of applied potential. This figure clearly shows two Nernstian reduction processes each with $n = 1$ values and midpoint potentials of -475 mV (NHE) for heme reduction and -445 mV (NHE) for the core Fe^{3+} . The heme present in Av ferritin is seen to be 30 mV more difficult to reduce than the bulk Fe^{3+} within the core. The reduction potential for core reduction (-420 ± 20 mV) measured by microcoulometry is slightly more positive than that for the same process measured spectroelectrochemically (-445 mV) as shown in Figure 2. We feel that the microcoulometrically determined value (-420 mV) may be more accurate because the procedure is simpler, the reduction change is larger and easier to measure, and no corrections are required.

Av Apobacterioferritin. The last entry in Table I presents analytical data for apo Av ferritin prepared by exhaustive dialysis against thioglycolic acid followed by dialysis against buffer. No phosphate was detected and the heme content remained unchanged compared to Av holoferritin at 1 heme per 2 subunits or 12 hemes per molecule. The iron content of this sample and others we have prepared differs only slightly from that expected from the iron-containing hemes.

The redox properties of Av apoferritin differ significantly from core-containing Av ferritin. The reaction of the heme groups with MV or $\text{S}_2\text{O}_4^{2-}$ is instantaneous compared to the same reaction with Av holoferritin which requires minutes and

Table II: Selected Mössbauer Parameters

material	T (K)	δ^a (mm/s)	ΔE_Q^b (mm/s)	ϵ^c	H_{hf}^d (kOe)	ref
Av ferritin	4.2	0.45		-0.01	490	this work
	80	0.48	0.78			this work
80% reduced Av ferritin	80	0.47	0.66			this work
		1.28	2.88			
mammalian ferritin	100	0.45	0.72			Watt et al. (1985)
	4.2	0.49		-0.03	502	
50% reduced mammalian ferritin	100	0.47	0.67			Watt et al. (1985)
		1.25	2.88			
	4.2	0.50		-0.03	501	
		1.40	3.13			
<i>Molpadia</i> granules	4.2	0.43		-0.01	420	Ofer et al. (1981)
polysaccharide-iron complex	12.8		0.9	-0.03	490	Berg et al. (1984)
	295		0.75			
<i>E. coli</i> ferritin					430	Bauminger et al. (1980)

^a Isomer shift relative to iron metal at room temperature. ^b Quadrupole splitting. Average line widths of ferric sites, $\Gamma \sim 0.45$ mm/s, and ferrous sites, $\Gamma \sim 0.55$ mm/s, indicate a distribution in the quadrupole splittings and isomer shifts. ^c Quadrupole perturbation of the magnetic hyperfine spectra, defined experimentally as $(d_2 - d_1)/4$ where Δ_1 and Δ_2 are the differences in millimeters per second between the two lowest energy absorption lines and the two highest energy absorption lines, respectively. ^d Saturation hyperfine magnetic field.

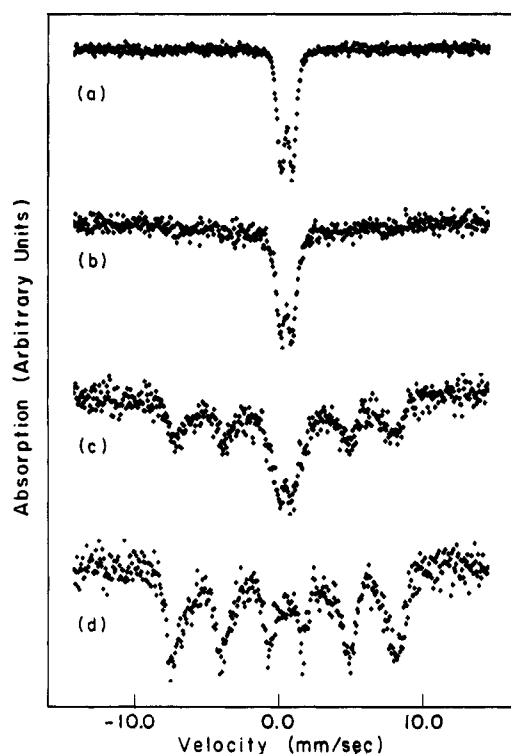


FIGURE 3: Mössbauer spectra of Av ferritin at (a) 80, (b) 20, (c) 10, and (d) 4.2 K.

hours, respectively, for complete reaction. The redox potential for Av apoferritin was measured by the microcoulometric method at pH 8.0 and found to be -225 mV (NHE). This result and that obtained for Av holoferritin shown in Figure 2 indicate that Av apoferritin is easier to reduce than Av holoferritin by 250 mV. The presence of the Fe^{3+} core has a significant effect on both the kinetic and redox properties of the protein-bound heme groups and suggests some type of core-heme interaction.

Mössbauer Spectroscopy of Av Ferritin. Mössbauer spectra of oxidized Av ferritin containing an average of 1000 Fe atoms per molecule were obtained between 4.2 and 250 K (Figure 3). Since heme iron constitutes only about 1% of iron in the molecule, it was not resolved from the core iron. For $30\text{ K} \leq T \leq 250\text{ K}$, the spectrum consists of a broadened quadrupole doublet with an isomer shift and quadrupole splitting characteristic of Fe^{3+} (Table II). At 4.2 K, the spectrum is a magnetic hyperfine sextet. Between 4.2 and 30 K, the spectrum consists of the quadrupole doublet superposed on the

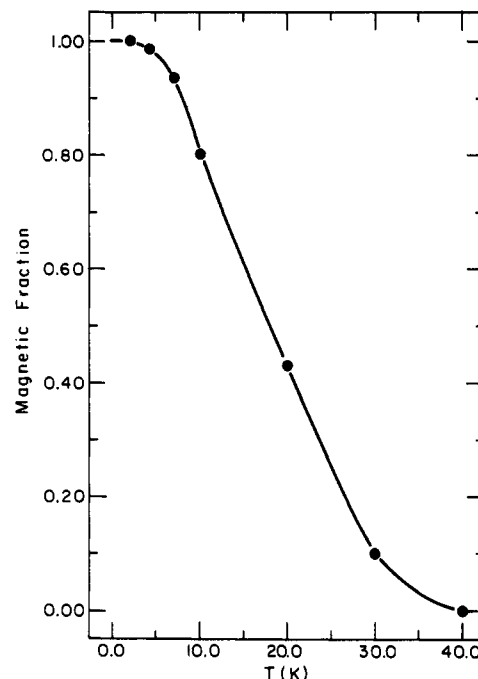


FIGURE 4: Magnetic fraction in Av ferritin, defined as the area under the six-line spectrum divided by the area under the total spectrum, plotted as a function of temperature. The solid line is drawn through the data.

magnetic hyperfine sextet, with relative intensities that increase and decrease, respectively, with increasing temperature. The magnetic fraction, defined as the ratio of the spectral intensity of the sextet to the sum of the sextet and doublet intensities, is shown plotted as a function of temperature in Figure 4.

The breadths of the outer lines of the 4.2-K sextet spectrum compared to the inner lines indicate a distribution of magnetic hyperfine fields. Moreover, there is a slight asymmetry in line shapes and positions that indicates a quadrupole perturbation of the magnetic hyperfine splitting. The 4.2-K spectrum was fitted as described by Ofer et al. (1981), yielding the magnetic field distribution shown in Figure 5, with a quadrupole interaction $\epsilon = -0.01$ mm/s. The mode of the magnetic hyperfine field distribution was 490 kOe, and the average value was 476 kOe. The mode of the distribution decreases to 485, 478, and 462 kOe at 10, 13.5, and 18 K, respectively.

The temperature dependence of the Mössbauer spectrum of Av ferritin is comparable to that of oxidized mammalian ferritin and is characteristic of the superparamagnetic behavior of the protein cores (Oosterhuis & Spartalian, 1976). Su-

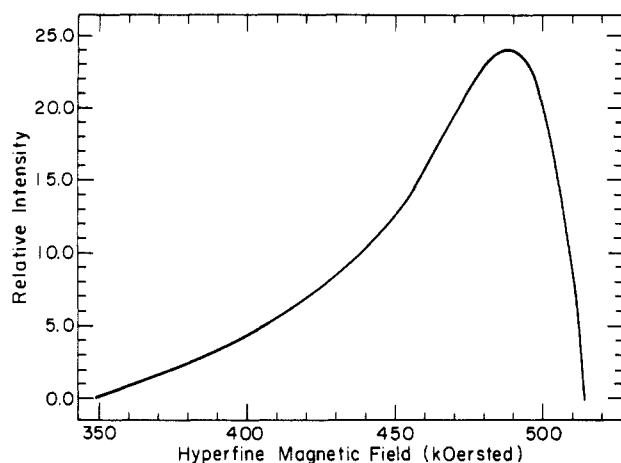


FIGURE 5: Hyperfine magnetic field distribution in Av ferritin at 4.2 K obtained by fitting the spectrum with a set of discrete magnetic field components.

perparamagnetism is a phenomenon that occurs in small particles of magnetically ordered materials in which transitions of the sublattice magnetizations between energetically equivalent crystallographic directions, that are the easy axes of magnetization in the material, are thermally activated. As the temperature increases, the sublattice transition frequency, ν , increases. ν is given by the equation:

$$\nu = \nu_0 \exp(-KV/kT) \quad (1)$$

where ν_0 is a constant of the order of 10^9 s^{-1} , K is the magnetic anisotropy energy per unit volume, V is the volume of the particle, and k is Boltzmann's constant. When ν is equal to or greater than ν_L (the nuclear Larmor precession frequency) in the magnetic hyperfine field H_{hf} , the Mössbauer sextet collapses to a quadrupole doublet. ν_L is given by

$$\nu_L = g_n \mu_n H_{\text{hf}} / h \quad (2)$$

with g_n the nuclear g factor, μ_n the nuclear magneton, and h Planck's constant. The temperature at which $\nu = \nu_L$ is called the blocking temperature, T_B . For $T > T_B$, $\nu > \nu_L$ and the Mössbauer spectrum consists of the doublet. For $T < T_B$, $\nu < \nu_L$ and the spectrum consists of the sextet. If all the protein cores had the same volume, the condition $\nu = \nu_L$ would be satisfied for all nuclei at the same blocking temperature, neglecting the possible variation in H_{hf} from the center to the surface of the core. However, a distribution in core volumes results in a distribution of blocking temperatures and hence an interval of temperature over which the doublet and sextet coexist.

The spectral parameters and temperature dependence of the Mössbauer spectrum in Av ferritin are comparable with those in mammalian ferritins and hemosiderin (Bell et al., 1984; Williams et al., 1978) and in polysaccharide-coated ferrihydrite particles (Berg et al., 1984). The major difference is in the average blocking temperatures, $\langle T_B \rangle$, operationally defined as the temperature at which the doublet and sextet intensities are equal. From Figure 4, $\langle T_B \rangle$ for Av ferritin is about 20 K. In human spleen ferritin and hemosiderin, Bell et al. (1984) report $\langle T_B \rangle = 38$ and 71 K, respectively. According to eq 1, if the magnetic anisotropy energy were equal in human ferritin and in Av ferritin, we would expect the average core volume of the former to be about twice the latter. Electron microscopy shows that the average core diameter in Av bacterioferritin is $\sim 55 \text{ \AA}$ (Stiefel & Watt, 1979), whereas for human spleen ferritin it is 60–65 \AA . This suggests that the magnetic anisotropy in Av ferritin may be somewhat less than in human ferritin. Differences in magnetic anisotropy could correspond

to differences in core chemical, structural, or surface properties and might reflect the higher phosphate (P_i) to Fe ratio and poorer core crystallinity of Av ferritin compared to human ferritin. These differences might account for a more rapid decrease in the mode of the magnetic hyperfine field distribution and a smaller quadrupole perturbation in Av ferritin than in human ferritin (Bell et al., 1984) and ferrihydrite (Williams et al., 1978). Poorer crystallinity could result in a decreased Néel temperature and poorer definition of the angle between the principal component of the electric field gradient and the magnetic hyperfine field in the core. Amorphous hydrous iron oxide granules with high phosphate from invertebrate dermis have lower magnetic hyperfine fields, a smaller quadrupole perturbation, and a lower Néel temperature than the ferritins and ferrihydrite (Ofer et al., 1981; see Table II).

Ferritin-like molecules have also been isolated from other prokaryotes including *E. coli* (Ec) (Bauminger et al., 1980) and *Pseudomonas aeruginosa* (Pa) (St. Pierre et al., 1984). In the Pa ferritin, the average core diameter is 60–65 \AA (Mann et al., 1986). At 1 K, the Mössbauer spectra of these materials are magnetic hyperfine sextets corresponding to a distribution of magnetic hyperfine fields with a mode of 430 kOe. As T increases between 1 and 3.5 K, the mode of the distribution decreases and collapses into the quadrupole doublet. This collapse of the hyperfine field suggests a magnetic phase transition rather than superparamagnetic relaxation, or a situation in which the Néel temperature is of the same order as the blocking temperature. Both Pa ferritin (Mann et al., 1986) and Av ferritin have high P_i/Fe ratios and poorly crystalline core structures. We suggest that the differences in magnetic properties might reflect differences in iron density in the cores and/or in the relative number of $\text{Fe}^{3+}\text{-O-Fe}^{3+}$, $\text{Fe}^{3+}\text{-OH-Fe}^{3+}$, and $\text{Fe}^{3+}\text{-OPO}_2\text{O-Fe}^{3+}$ bridges in the two materials. Hydroxide bridges have generally lower exchange constants and lower hyperfine fields than oxide bridges.

Mössbauer Spectroscopy of Partially Reduced Av Ferritin. Mössbauer spectra of Av ferritin containing approximately 1000 Fe atoms average per molecule and reduced by 0.8 electron per iron atom were recorded for sample temperatures between 2 and 250 K. Representative spectra are shown in Figure 6. The spectra for sample temperatures above 30 K can all be decomposed into overlapping quadrupole doublets corresponding to Fe^{3+} and Fe^{2+} in the cores. The ferric doublet isomer shift and quadrupole splitting listed in Table II are similar to those of Fe^{3+} in oxidized Av ferritin and vary only slightly between 30 and 250 K. The ferrous quadrupole doublet isomer shift and quadrupole splitting in Table II are comparable to Fe^{2+} in reduced mammalian ferritin. The ferrous quadrupole splitting decreases by about 10% between 30 and 250 K. At 60 K, Fe^{3+} and Fe^{2+} doublets constitute 20% and 80%, respectively, of the total spectral intensity, reflecting the degree of reduction of the core. At higher temperatures, both the Fe^{3+} and Fe^{2+} quadrupole doublet intensities are decreased (Figure 7), but the Fe^{2+} intensity decreases more rapidly with increasing temperature than the Fe^{3+} intensity. This means that the Fe^{2+} ions have a more temperature-sensitive recoilless fraction than the Fe^{3+} ions. Higher temperature sensitivity of the recoilless fraction probably reflects looser binding of the Fe^{2+} ions than Fe^{3+} ions in the Av ferritin core. The temperature dependence of the recoilless fraction of Fe^{3+} in the partially reduced sample is similar to that of Fe^{3+} in the oxidized sample.

Below 30 K, the ferric subspectrum consists of the quadrupole doublet superposed on a magnetic hyperfine sextet with

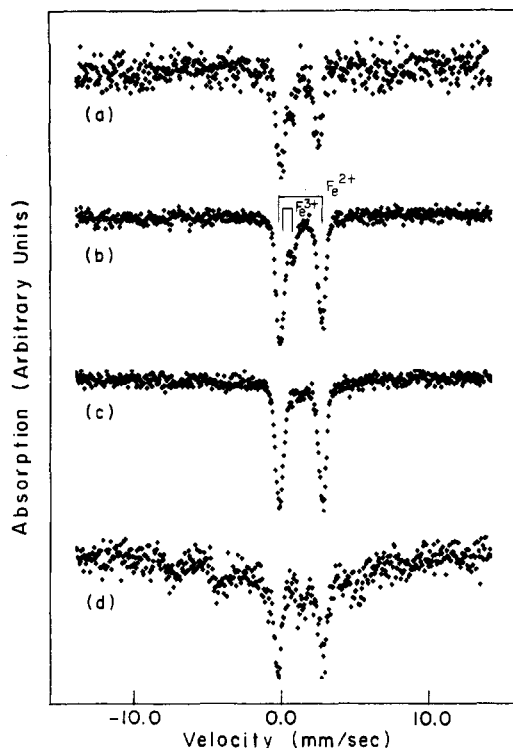


FIGURE 6: Mössbauer spectra of 80% reduced Av ferritin at (a) 230, (b) 80, (c) 20, and (d) 2 K.

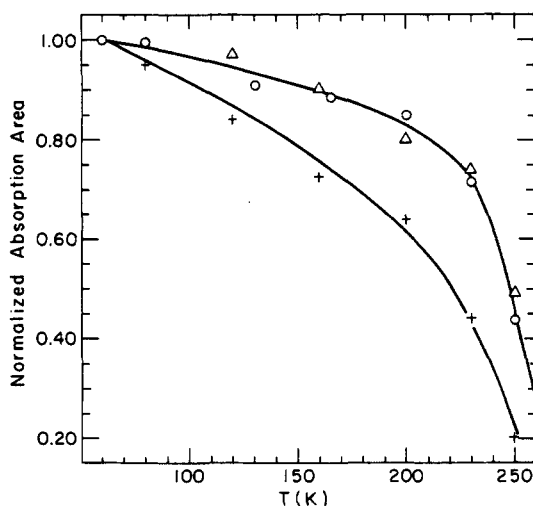


FIGURE 7: Quadrupole doublet area, normalized to the doublet area at 60 K, plotted as a function of temperature for (O) Fe^{3+} in Av ferritin, (Δ) Fe^{3+} in 80% reduced Av ferritin, and (+) Fe^{2+} in 80% reduced Av ferritin. The solid lines are drawn through the data.

relative intensities that are temperature dependent. This is similar to the spectrum of oxidized Av ferritin below 30 K. However, because of the low percentage of Fe^{3+} in the partially reduced samples, it is difficult to resolve the sextet spectrum. Nevertheless, it is possible to follow the temperature dependence of the intensity of the Fe^{3+} quadrupole doublet. Whereas the Fe^{3+} doublet intensity at 20 K in oxidized Av ferritin is about 50% of its value at 60 K, the Fe^{3+} doublet intensity in the partially reduced sample is less than 50% of its value at 60 K. This means that more of the Fe^{3+} intensity in the partially reduced sample is in the sextet at 20 K compared to the oxidized sample. Since at any temperature the ferric doublet and sextet correspond to smaller and larger particles, respectively, this suggests that the apparent particle size distribution for the ferric ions in the partially reduced sample is displaced toward a larger average size. If electrons entered

all the bacterioferritin molecules at the same rate, the average Fe^{3+} particle size would decrease; hence, an increased average particle size suggests that the Av ferritin molecules with smaller numbers of iron atoms are preferentially reduced. A similar effect has been noted in partially reduced mammalian ferritin (Watt et al., 1985).

The Fe^{2+} quadrupole doublet intensity at 10 K is approximately the same as at 60 K. Below 10 K, the doublet intensity is decreased and is superposed on a broad ($\Gamma = 8$ mm/s), unresolved spectrum, suggesting magnetic interactions between some of the Fe^{2+} ions. Some of the quadrupole doublet intensity persists even at 2 K. This could mean that some of the Fe^{2+} ions are bound as isolated ions or as spin-coupled pairs with singlet ground states.

DISCUSSION

In the absence of Fe^{2+} chelators, electron transfer from external reductants converts the core Fe^{3+} to Fe^{2+} in both mammalian and bacterial ferritin with complete retention of the resulting Fe^{2+} within the protein interior. This simple procedure provides a means for preparing partially or completely reduced ferritin cores containing discrete Fe^{2+} in either mammalian (Watt et al., 1985) or bacterial (Stiefel & Watt, 1979) ferritins. In their core reduction properties, both ferritins are very similar; however, the bacterial ferritin obtained from *Azotobacter vinelandii* differs in significant ways from mammalian ferritin even though both proteins have a number of properties in common (Stiefel & Watt, 1979). The data in Table I clearly show that Av ferritin has a high phosphate content ranging from near 0.5 to 1.0 $\text{P}_i/\text{core Fe}$, values much higher than that of 0.1 P_i/Fe reported for mammalian ferritin. The increased stability of the Fe^{2+} core, the different redox properties, and the greatly different proton uptake capability observed upon reduction of Av ferritin suggest a significantly different core character compared to that in mammalian ferritin (Watt et al., 1985). The high phosphate level in the core matrix may be the determining factor for these differences in core behavior. Although the data in Table I suggest a trend of increasing P_i content with decreasing Fe loading in Av ferritin, this trend, if real, is not manifested in any of the physicochemical core properties that we have so far investigated as the P_i and Fe levels vary.

The presence of heme in bacterial ferritin raises a number of questions regarding its purpose and its relationship with the core. The quite constant stoichiometry of 0.5 heme/subunit suggests a relationship of one heme being shared between two subunits, but the significance of this possibility remains unclear. The report by Yariv et al. (1981) that *E. coli* ferritin binds additional heme could indicate either that our Av samples had lost heme during preparation or that it does not bind its full complement of heme during the particular growth conditions used. The constancy of heme content for the samples listed in Table I and similar results obtained from Av ferritin samples prepared by quite different isolation procedures suggest that 0.5 heme/subunit may be the true composition of native Av ferritin. Further insights regarding possible roles for the heme in Av ferritin can be gained by considering the redox properties of Av ferritin.

Figure 1 demonstrates that both the core Fe^{3+} and the heme groups are capable of redox reactions with a common reductant. There is a clear preference in redox reactivity, with the core Fe^{3+} initially undergoing reduction with the MV reductant followed by heme reduction. Similar results were obtained with $\text{S}_2\text{O}_4^{2-}$ as reductant, but the reactions are much slower in this case. An interesting question arises when considering Figure 1. Are the results shown a consequence of separate

reaction of the reductant with each type of redox center present or do the results suggest an electron transfer sequence in which the reductant first reduces the heme which in turn transfers electrons to core Fe^{3+} ? The results in Figure 2 showing that the heme is 30 mV more difficult to reduce than the core Fe^{3+} are consistent with both types of centers being simultaneously reducible. As reductant is added, as in Figure 1, the most easily reducible center would undergo reaction first followed by the next most reducible center. Figure 2 predicts that the preferred sequence would be core Fe^{3+} followed closely by heme reduction, the result observed in Figure 1.

However, an alternate view is that core Fe^{3+} reduction by external reductants does not occur directly but is mediated by the heme groups. The results of Figure 1 can be interpreted on this basis by assuming that the reductant initially added first, exclusively reduces the heme which subsequently transfers electrons to the core. Complete heme oxidation by this last step at low initial reductant ratios occurs, as shown in Figure 1, because (1) the heme to core Fe^{3+} electron transfer is driven by a favorable 30-mV potential and (2) the electron acceptance capacity of the core is so extensive (core Fe^{3+} /heme > 100/1) that as much as 20% core Fe^{3+} reduction can occur before appreciable heme reduction is detected. A distinction between these possibilities cannot be made from our data but is clearly of importance in understanding the redox nature of the core Fe^{3+} and heme groups on Av ferritin.

Related to the reducibility of the Av ferritin core is the question of concerted proton transfer. We have previously reported that the reduction of mammalian ferritin core Fe^{3+} is accompanied by the transfer of $2 \text{ H}^+/\text{e}^-$. This proton transfer was determined directly from pH measurements and from the decrease in core Fe^{3+} reduction potential with decreasing pH. No such reduction potential variation with pH was encountered with Av ferritin, except at pH 6.0, suggesting the lack of proton involvement with core Fe^{3+} reduction. This demonstrates a significant difference between the core properties of Av ferritin and mammalian ferritin, a result also suggested by the high P_i content of the former relative to the latter. If the Av ferritin is indeed an analogous iron storage protein in bacteria, the results so far obtained suggest that the methods of Fe storage and release may differ significantly from those in the mammalian system.

Av apoferritin is readily prepared with all core Fe^{3+} removed but with all original heme groups remaining. The removal of the core causes a greatly increased rate of heme reduction. The redox potential undergoes a positive 250-mV shift in the absence of the core, making the hemes easier to reduce in the apo form than in the holo form. These results suggest a significant core-heme interaction when both protein constituents are present in the holo Av ferritin, sufficient to alter both the kinetic and thermodynamic properties of the bound heme groups.

Mössbauer spectroscopy of oxidized Av ferritin indicates that the cores consist of antiferromagnetically coupled, high-spin Fe^{3+} which exhibits superparamagnetic behavior at low temperatures. In this respect, Av ferritin is similar to mammalian ferritin, except that the average blocking temperatures are less in Av ferritin. This might reflect the higher phos-

phate/ Fe^{3+} ratio and poorer crystallinity in Av ferritin. Reduction of Av ferritin results in the presence of Fe^{2+} in the core. Fe^{2+} and Fe^{3+} ions in partially reduced samples have different temperature dependences of their recoilless fractions and different temperature dependences of their magnetic hyperfine interactions. Taken together with the apparent increase in the average Fe^{3+} particle size in the partially reduced samples, this suggests that Fe^{2+} ions form a separate phase in the Av ferritin cores and that cores containing less iron atoms are preferentially reduced. The properties of reduced iron in Av ferritin are very similar to those of reduced iron in mammalian ferritin (Watt et al., 1985).

Ferritin is an important example of a biomineralization process in which an inorganic mineral phase is deposited on or in a biomacromolecular structure. We have shown significant differences between ferritins from different sources, suggesting differences in the protein-mineral interaction or, more likely, differences in structure and reactivity of the different mineral phases. Further study of the chemical, structural, and electrochemical nature of these biomolecules will be required to fully understand these differences and to elucidate the nature of their redox and chemical behavior in a physiologically meaningful context.

Registry No. Fe, 7439-89-6; heme *b*, 14875-96-8.

REFERENCES

- Bauminger, E. R., Cohen, S. G., Dickson, D. P. E., Levy, A., Ofer, S., & Yariv, J. (1980) *Biochim. Biophys. Acta* 623, 237.
- Bell, S. H., Weir, M. P., Dickson, D. P. E., Gibson, J. F., Sharp, G. A., & Peters, T. J. (1984) *Biochim. Biophys. Acta* 787, 227.
- Berg, K. A., Bowen, L. H., Hedges, S. W., Bereman, R. D., & Vance, C. T. (1984) *J. Inorg. Biochem.* 22, 125.
- Bulen, W. A., LeComte, J. R., & Lough, S. (1973) *Biochem. Biophys. Res. Commun.* 54, 1274.
- Heineman, W. R. (1978) *Anal. Chem.* 50, 390A.
- Mann, S., Bannister, J. V., & Williams, R. J. P. (1986) *J. Mol. Biol.* (in press).
- Ofer, S., Papaefthymiou, G. C., Frankel, R. B., & Lowenstam, H. A. (1981) *Biochim. Biophys. Acta* 676, 199.
- Oosterhuis, W. T., & Spartalian, K. (1976) in *Applications of Mössbauer Spectroscopy* (Cohen, R. L., Ed.) Vol. I, p 141, Academic Press, New York.
- Stiefel, E. I., & Watt, G. D. (1979) *Nature (London)* 279, 81.
- St. Pierre, T. G., Bell, S. H., Dickson, D. P. E., Mann, S., Webb, J., Moore, G. R., & Williams, R. J. P. (1986) (in press).
- Treffry, A., & Harrison, P. M. (1978) *Biochem. J.* 171, 313.
- Watt, G. D. (1979) *Anal. Biochem.* 99, 399.
- Watt, G. D., Frankel, R. B., & Papaefthymiou, G. C. (1985) *Proc. Natl. Acad. Sci. U.S.A.* 82, 3640.
- Williams, J. M., Danson, D. P., & Janot, Chr. (1978) *Phys. Med. Biol.* 23, 835.
- Yariv, J., Kalb, J., Sperling, R., Bauminger, E. R., Cohen, S. G., & Ofer, S. (1981) *Biochem. J.* 197, 171.